Change Detection in Multilook Polarimetric SAR Imagery with Hotelling-Lawley Trace and Determinant Ratio Test Statistics

Vahid Akbari[1] Nizar Bouhlel[2]
1 University of Stirling, UK
2 Institut Agro, Univ Angers, France

POLINSAR AND BIOMASS 2023, Toulouse, 19th June 2023

Change detection in matrix-variate data

- The scattering vecor is multilooked with L number of looks

$$\mathbf{s} = [s_{\mathrm{hh}}, s_{\mathrm{hv}}, s_{\mathrm{vh}}, s_{\mathrm{vv}}]^T \in \mathbb{C}^d$$

$$\mathbf{X} = \frac{1}{L}\sum_{\ell=1}^{L} \mathbf{s}_\ell \mathbf{s}_\ell^H, \quad L \geq d$$

- Let **X** and **Y** are independent and both bollows scaled complex Wishart distributions

$$p_{\mathbf{X}}(\mathbf{X}) = \frac{L^{Ld}|\mathbf{X}|^{L-d}}{\Gamma_d(L)|\mathbf{\Sigma}|^L} \exp\left(-L\mathrm{tr}(\mathbf{\Sigma}^{-1}\mathbf{X})\right)$$

$$\mathbf{X} \in s\mathcal{W}(L_x, \mathbf{\Sigma}_x) \text{ and } \mathbf{Y} \in s\mathcal{W}(L_y, \mathbf{\Sigma}_y)$$

Time 1

Time 2

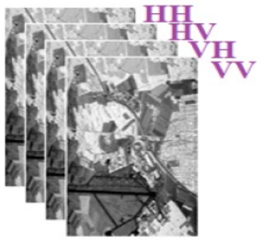

- Hyphothesis Testing

$$\begin{cases} H_0 : \mathbf{\Sigma}_x = \mathbf{\Sigma}_y \\ H_1 : \mathbf{\Sigma}_x \neq \mathbf{\Sigma}_y \end{cases}$$

Background

1. Wishart Likelihood tatio test (LRT) statistic

K. Conradsen, A. A. Nielsen, J. Schou, and H. Skriver, “A test statistic in the complex wishart distribution and its application to change detection in polarimetric SAR data,” IEEE Trans. Geosci. Remote Sens., vol. 41, no. 1, pp. 4–19, Jan. 2003

2. Complex-kind Hotelling Lawley Trace (HLT) statistic

Akbari, V., S.N. Anfinsen, A.P. Doulgeris and T. Eltoft , G. Moser, S. B. Serpico, Polarimetric SAR Change Detection with the Complex Hotelling-Lawley Trace Statistic, IEEE Trans. Geosci. Remote Sens., vol. 54, no. 7, pp. 3953–3966, Mar. 2016.

3. Determinant Ratio Test (DRT) statistic

N. Boulel, V. Akbari and S. Méric, “Change detection in multilook polarimetric SAR imagery with determinant ratio test statistic,” in IEEE Transactions on Geoscience and Remote Sensing, vol. 60, pp. 5200515-5200515,   2022.

1) Similary Measure: Likelihood Test Statistic

- Change detection test by LRT

$$\tau_{\mathrm{LRT}} = -2\rho \ln Q$$

where

$$Q = \frac{(L_x + L_y)^{d(L_x+L_y)}}{L_x^{dL_x} L_y^{dL_y}} \frac{|L_x \mathbf{X}|^{L_x} |L_y \mathbf{Y}|^{L_y}}{|L_x \mathbf{X} + L_y \mathbf{Y}|^{L_x+L_y}}.$$

- The distribution of the LRT statistic is approximated by

$$\tau_{\mathrm{LRT}} \sim \chi^2(d^2) + w_2[\chi^2(d^2+4) - \chi^2(d^2)]$$

and

$$\rho = 1 - \frac{2d^2 - 1}{6d}\left(\frac{1}{L_x} + \frac{1}{L_y} - \frac{1}{L_x + L_y}\right).$$

- The test with a desired Pfa is given by

$$\tau_{\mathrm{LRT}} \underset{H_0}{\overset{H_1}{\gtrless}} T$$

  - ➢ where the threshold T is determined

$$P_{\mathrm{fa}} = \int_T^{+\infty} f_{\tau_{\mathrm{LRT}}}(\tau | H_0) \mathrm{d}\tau.$$

K. Conradsen, A. A. Nielsen, J. Schou, and H. Skriver, "A test statistic in the complex wishart distribution and its application to change detection in polarimetric SAR data," IEEE Trans. Geosci. Remote Sens., vol. 41, no. 1, pp. 4–19, Jan. 2003

2) Similarity Measures: Hotelling-Lawley Trace

- Complex-kind Hotelling Lawley Trace (HLT) Statistic
- The exact distribution of the HLT statistic is difficult to derive
- The HLT is approximated by a Fisher-Snedecor Distribution
- Moments of HLT

$$\tau_{\mathrm{HLT}} = \mathrm{tr}(\mathbf{Y}^{-1}\mathbf{X}).$$

$$\begin{cases} H_0 : \mathbf{\Sigma}_x = \mathbf{\Sigma}_y \\ H_1 : \mathbf{\Sigma}_x \neq \mathbf{\Sigma}_y \end{cases}$$

$$\tau_{\mathrm{HLT}} \sim \mathrm{FS}(\xi, \zeta, \mu).$$

$$E\{\tau_{HL}\} = \frac{d}{L_x - d},$$

$$E\{\tau_{HL}^2\} = \left(\frac{L_y + 1}{L_y}\right) \frac{dL_x^2(d(L_x - d) + 1)}{(L_x - d)^3 - (L_x - d)},$$

$$E\{\tau_{HL}^3\} = \frac{L_x^3}{(L_x - d)^4}[d^3(L_x - d) + 3d^2 + \frac{3}{L_y}\left(d^2(L_x - d) + d(d^2 + 2)\right) + \frac{2}{L_y^2}\left(d(L_x - d) + 3d^2\right)],$$

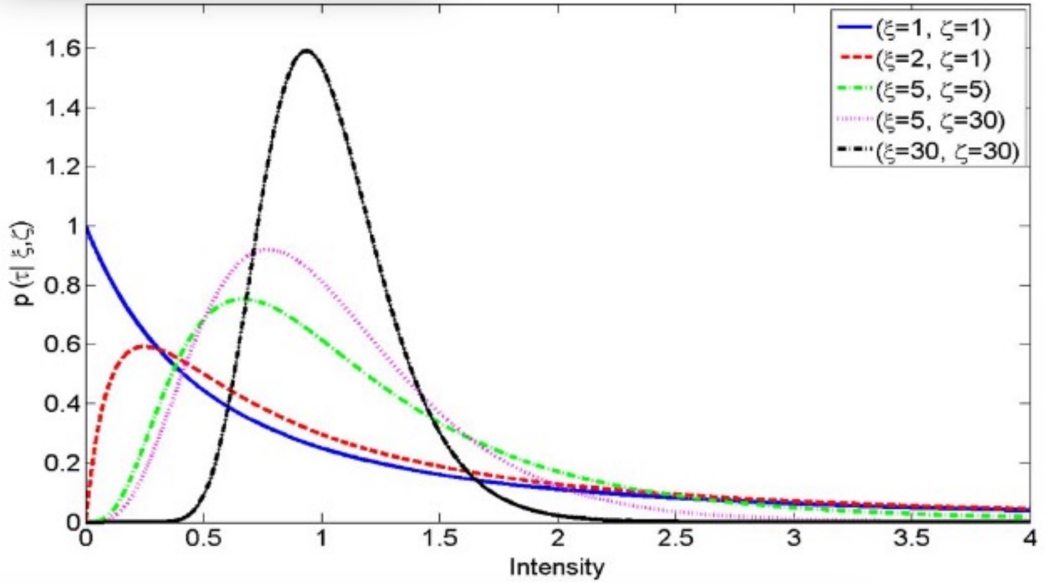

- Solution to estimate the FS paramters

$$m_\nu^{(\mathrm{FS})}(\xi, \zeta, \mu) = m_\nu^{(\mathrm{HLT})}(L_a, L_b, d), \qquad \nu = 1, 2, 3.$$

$$(\hat{\xi}, \hat{\zeta}) = \underset{(\xi,\zeta)}{\arg\min} \sum_{\nu=2}^{3} \left(m_\nu^{(\mathrm{FS})} - m_\nu^{(\mathrm{HLT})}\right)^2.$$

Akbari, V., S.N. Anfinsen, A.P. Doulgeris and T. Eltoft , G. Moser, S. B. Serpico, Polarimetric SAR Change Detection with the Complex Hotelling-Lawley Trace Statistic, IEEE Trans. Geosci. Remote Sens., vol. 54, no. 7, pp. 3953–3966, Mar. 2016.

HLT and CFAR-type thresholding

- The HLT test is not CFAR, but we use the CFAR principle to determine the threshold.
- Find a global estimation of Lx and Ly
- Generate the HLT statistics image using

$$\tau_{\mathrm{HLT}} = \mathrm{tr}(\mathbf{Y}^{-1}\mathbf{X}) \text{ and } \tau'_{\mathrm{HLT}} = \mathrm{tr}(\mathbf{X}^{-1}\mathbf{Y}) \rightarrow \max\{\tau_{\mathrm{HLT}}, \tau'_{\mathrm{HLT}}\}$$

- Compute the CFAR threshold for a specific Pfa

$$P_{\mathrm{fa}} = 2\int_{T}^{+\infty} f_{\tau_{\mathrm{HLT}}}(\tau|H_0)\mathrm{d}\tau.$$

- Apply the threshold and obtain the binary change detection map.

$$\max\{\tau_{\mathrm{HLT}}, \tau'_{\mathrm{HLT}}\} \underset{H_0}{\overset{H_1}{\gtrless}} T.$$

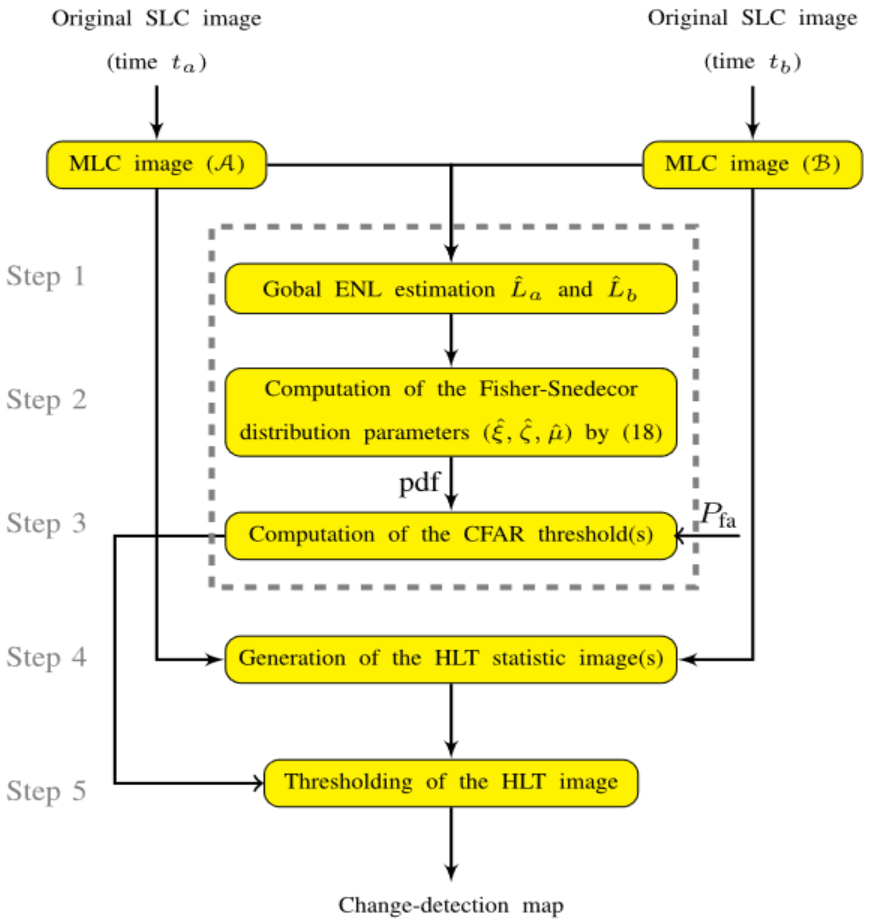

3) Similarity Measures: Determinant Ratio Test

- Determinant ratio test (DRT) statistic

$$\tau_{\text{DRT}} = \frac{|L_x \mathbf{X}|}{|L_y \mathbf{Y}|}.$$

$$\begin{cases} H_0 : \mathbf{\Sigma}_x = \mathbf{\Sigma}_y \\ H_1 : \mathbf{\Sigma}_x \neq \mathbf{\Sigma}_y \end{cases}$$

- Distinct ENLs $L_x \neq L_y$

- The exact distribution of the DRT statistic is Wilks's lambda distribution of the second kind

$$\tau_{\text{DRT}} \sim \Lambda'(L_x + L_y, d, L_y).$$

➢ If $L_x = L_y = L$ → $\tau_{\text{DRT}} = \frac{|\mathbf{X}|}{|\mathbf{Y}|} \sim \Lambda'(2L, d, L).$

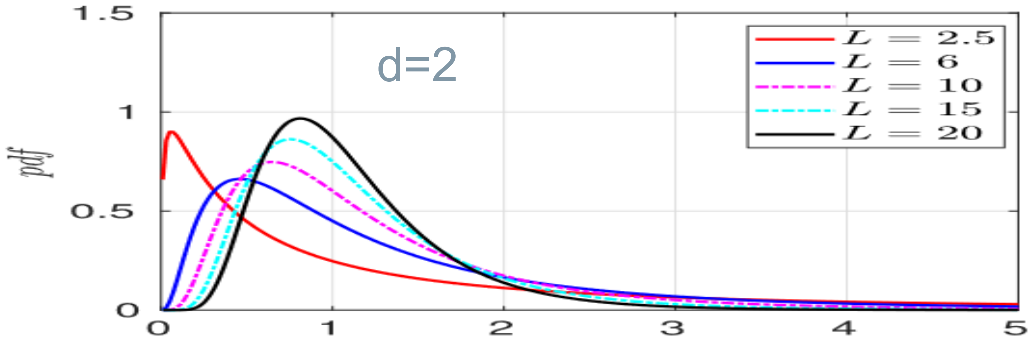

(a)

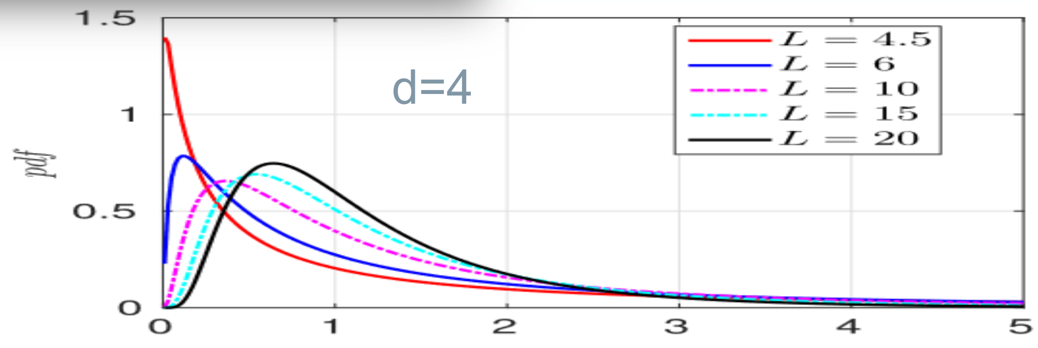

(b)

N. Boulel, V. Akbari and S. Méric, "Change detection in multilook polarimetric SAR imagery with determinant ratio test statistic," in IEEE Transactions on Geoscience and Remote Sensing, vol, 60, pp. 5200515-5200515, 2022.

DRT and CFAR Thresholding

- Find a global estimation of Lx and Ly
- Generate the DRT statistics image using

$$\tau_{\mathrm{DRT}} = \frac{|L_x \mathbf{X}|}{|L_y \mathbf{Y}|}, \quad \text{and } \tau'_{\mathrm{DRT}} = \frac{|L_y \mathbf{Y}|}{|L_x \mathbf{X}|}.$$

$$\max\left\{\tau_{\mathrm{DRT}}, \tau'_{\mathrm{DRT}}\right\}$$

- Compute the CFAR threshold for a specific Pfa

$$P_{\mathrm{fa}} = 2\int_{T}^{+\infty} f_{\tau_{\mathrm{DRT}}}(\tau \mid H_0)\,\mathrm{d}\tau.$$

- Apply the threshold and obtain the binary change detection map.

$$\max\left\{\tau_{\mathrm{DRT}}, \tau'_{\mathrm{DRT}}\right\} \underset{H_0}{\overset{H_1}{\gtrless}} T.$$

Experimental Results: Simulated PolSAR data

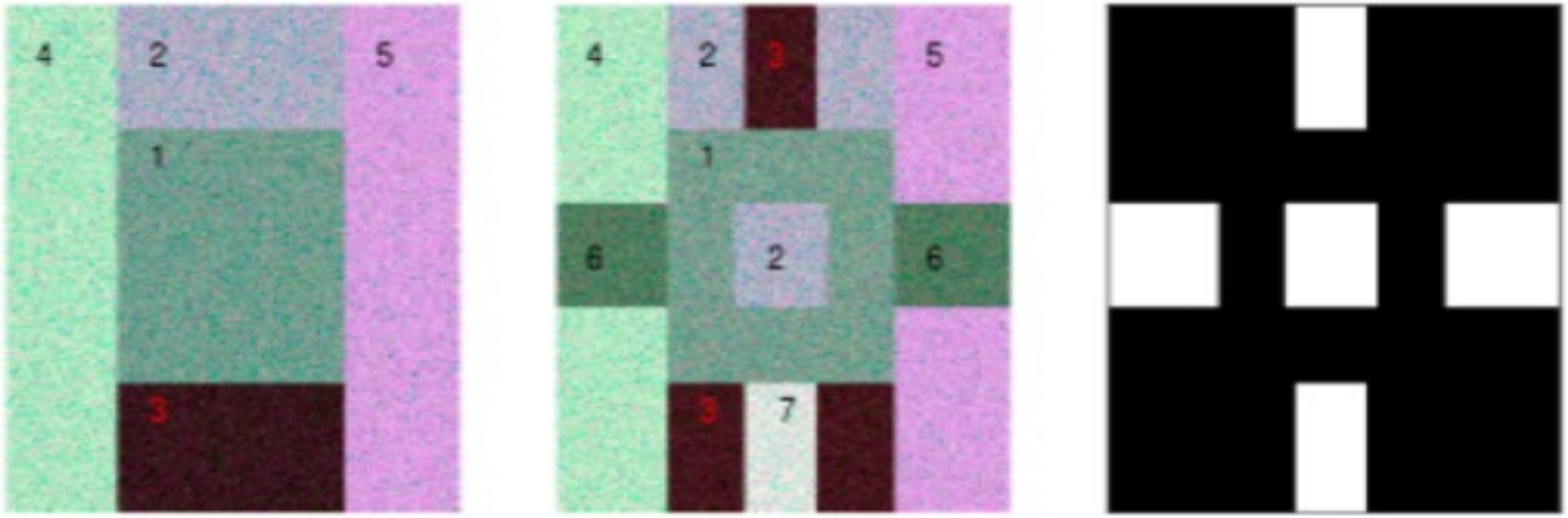

(a) (b) (c)

Area	$\{\Sigma_{11}, \Sigma_{22}, \Sigma_{33}, \Sigma_{44}, \Sigma_{12}, \Sigma_{13}, \Sigma_{14}, \Sigma_{23}, \Sigma_{24}, \Sigma_{34}\} \times 10^{-3}$
1	2.6, 0.6, 0.6, 2.9, 0, 0, 0.9-1.2i, 0, 0, 0
2	11.9, 1, 1, 7.7, 0, 0, -2.1-3.6i, 1, 0, 0, 0
3	0.28, 0.007, 0.007, 0.073, 0, 0, 0.13-0.004i, 0, 0, 0
4	6.7, 6, 6, 11.2, 0, 0, 2.2+0.8i, 0, 0, 0
5	27.3, 0.6, 0.6, 12, 0, 0, 14.2-6.4i, 0, 0, 0
6	1, 0.2, 0.2, 0.8, 0, 0, 0.5-i, 0, 0, 0
7	8.9, 5.5, 5.5, 26.1, 0, 0, -1.1+0.2i, 0, 0, 0

Experimental Results: Simulated PolSAR data (L=8)

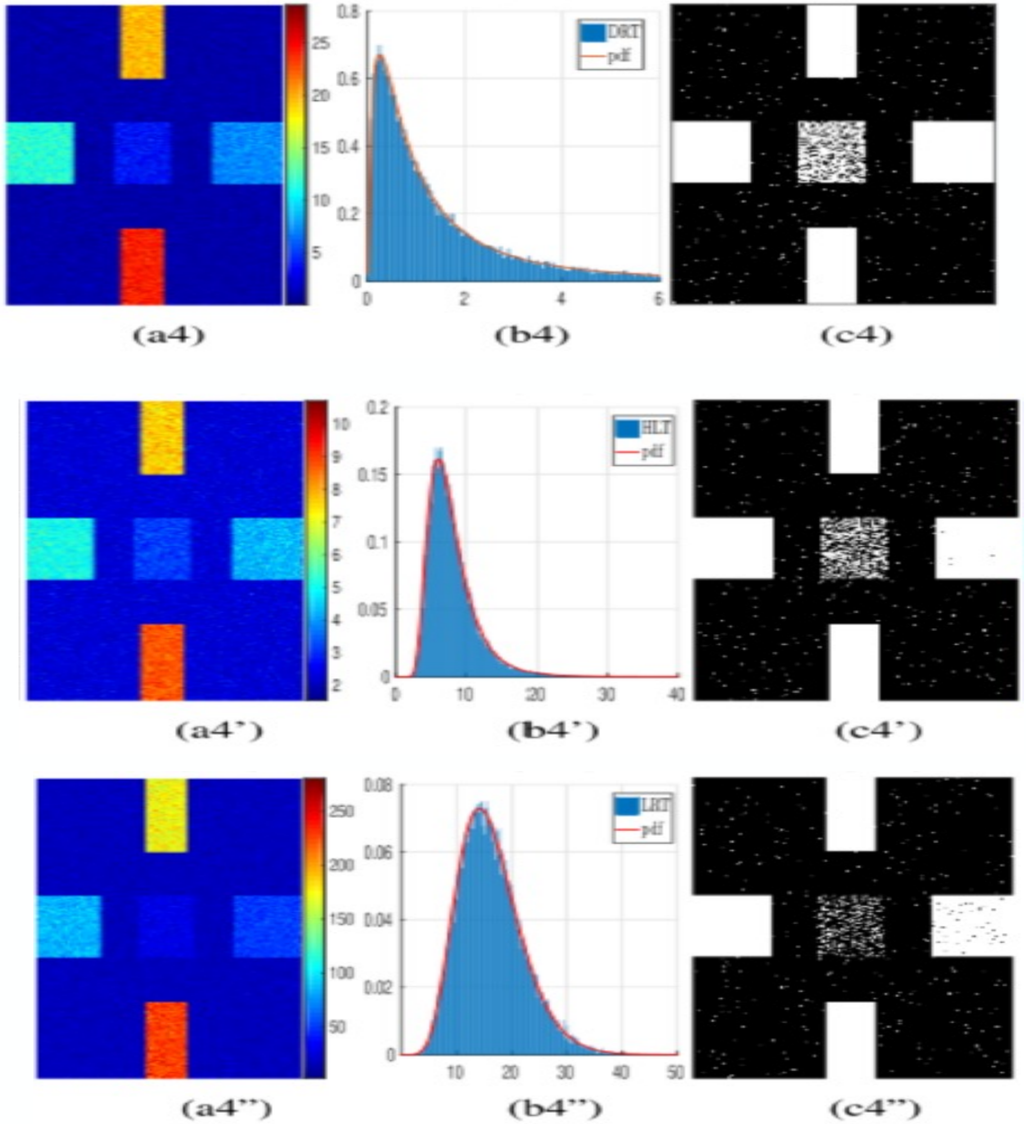

Looks	Specified FAR(%)	Method	Measured FAR (%)	Detection rate (%)	Overall error rate (%)
8	0.5	DRT	0.46	92.86	1.94
		HLT	0.58	87.97	3.12
		LRT	0.44	83.23	4.07
	1	DRT	1.00	94.60	1.98
		HLT	1.13	90.33	3.02
		LRT	0.95	85.25	4.02
	5	DRT	5.22	97.88	4.53
		HLT	5.07	95.79	4.88
		LRT	5.02	90.97	5.91
	10	DRT	10.23	98.85	8.21
		HLT	9.77	97.65	8.12
		LRT	10.18	93.89	9.27

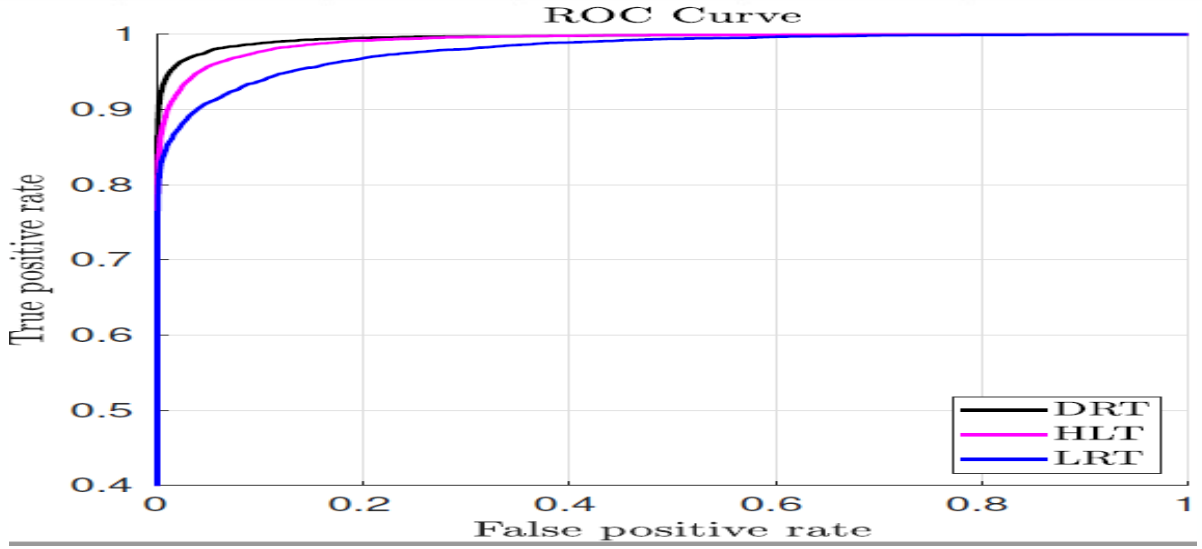

Experimental Results: RADARSAT-2 Images (L=24)

24 looks, Lx=7.2, Ly=6.9

T1: April 2009 | T2: June 2010 | Ground Truth

(a) (b) (c)

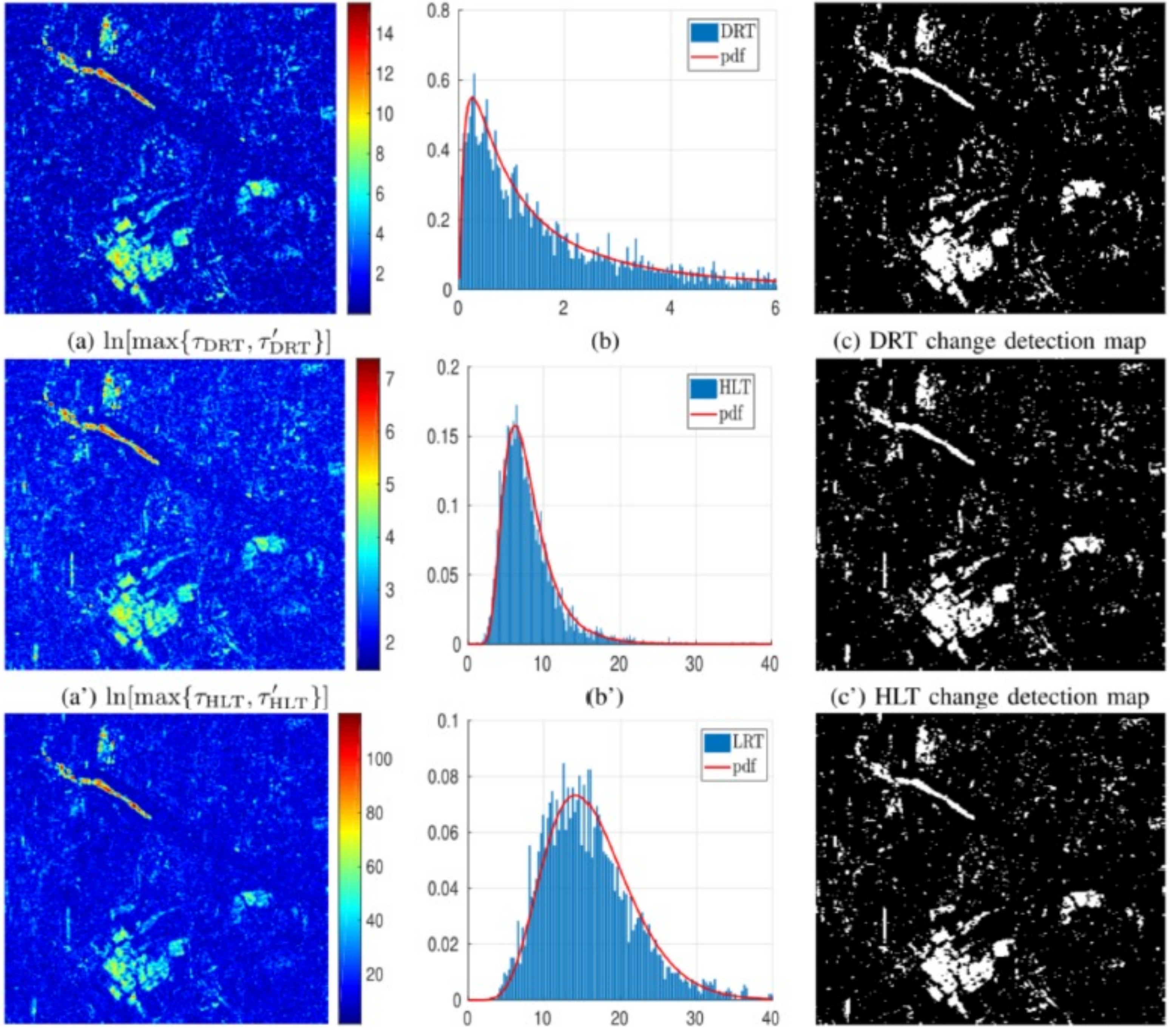

(a) $\ln[\max\{\tau_{\mathrm{DRT}}, \tau'_{\mathrm{DRT}}\}]$ (b) (c) DRT change detection map

(a') $\ln[\max\{\tau_{\mathrm{HLT}}, \tau'_{\mathrm{HLT}}\}]$ (b') (c') HLT change detection map

(a'') τ_{LRT} (b'') (c'') LRT change detection map

Specified FAR(%)	Method	Measured FAR (%)	Detection rate (%)	Overall error rate (%)
0.5	DRT	0.91	95.53	1.98
	HLT	0.61	90.90	3.16
	LRT	1.11	92.50	3.03
1	DRT	1.40	96.36	2.07
	HLT	1.10	93.56	2.71
	LRT	1.73	94.17	2.96
5	DRT	5.24	98.63	4.07
	HLT	4.03	97.42	3.59
	LRT	5.70	97.50	4.74
10	DRT	9.60	99.24	6.94
	HLT	7.03	98.56	5.35
	LRT	9.77	98.41	7.31

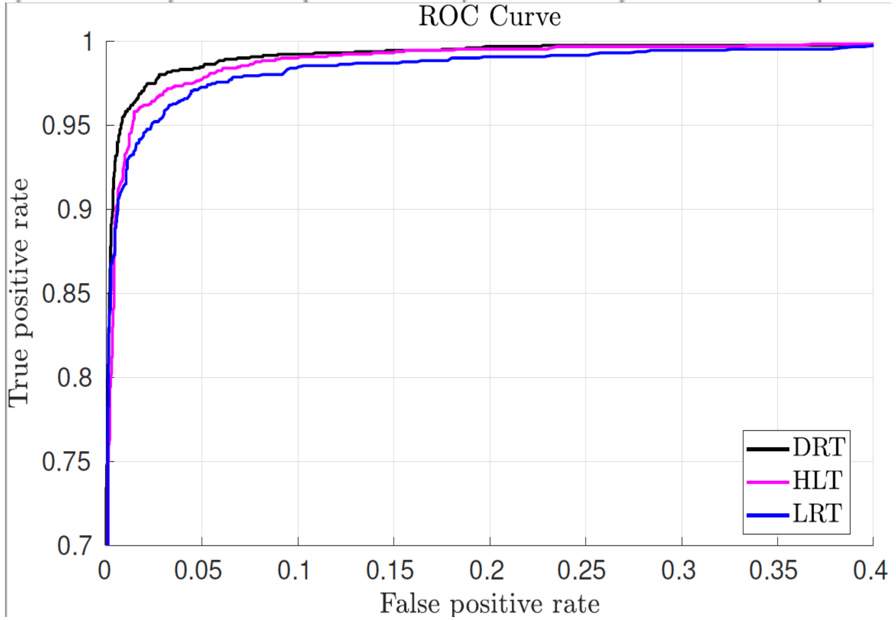

Experimental Results: UAVSAR Images (L=6)

T1: April 2009

T2: May 2015

Ground Truth

(a)

(b)

(c)

Experimental Results: UAVSAR Images (L=6)

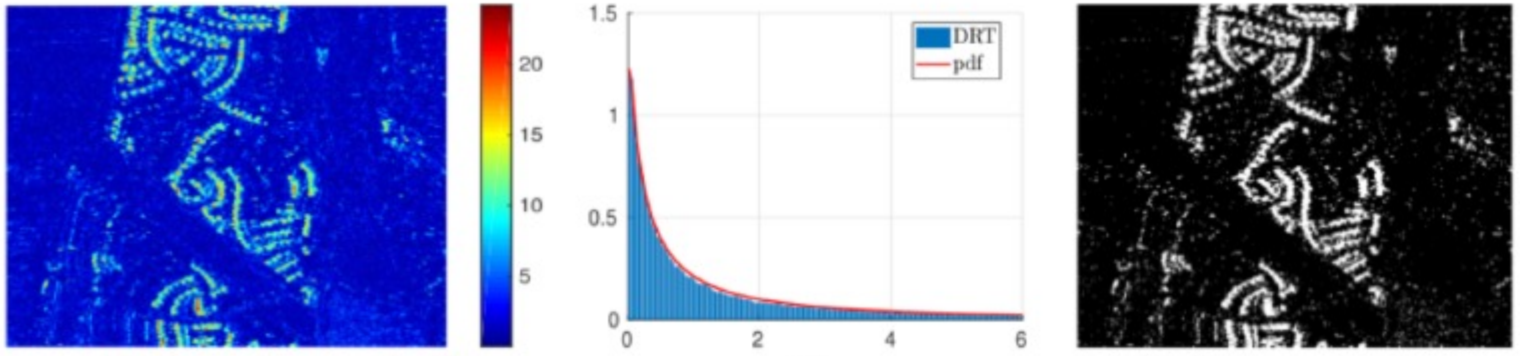

(a1) $\ln[\max\{\tau_{DRT}, \tau'_{DRT}\}]$ (b1) (c1) DRT change detection map

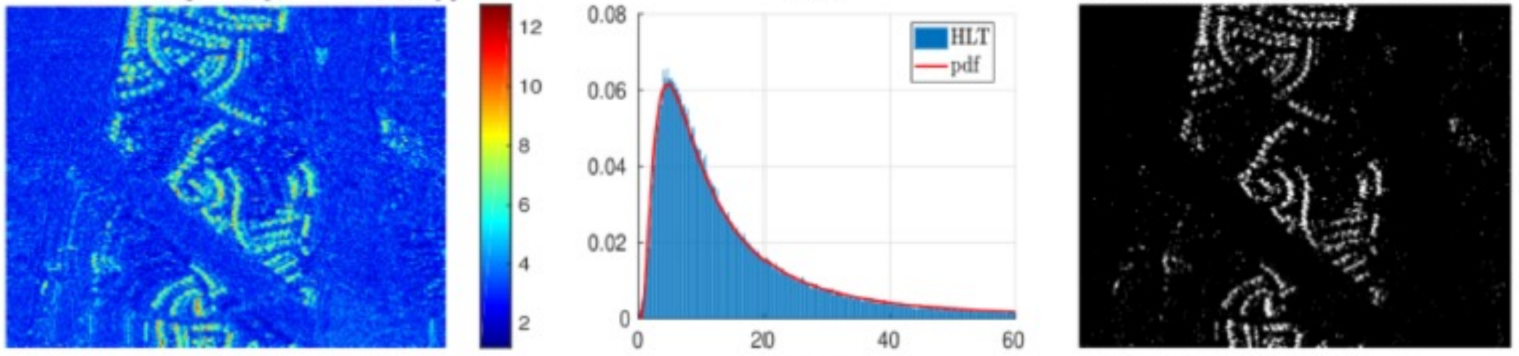

(a1') $\ln[\max\{\tau_{HLT}, \tau'_{HLT}\}]$ (b1') (c1') HLT change detection map

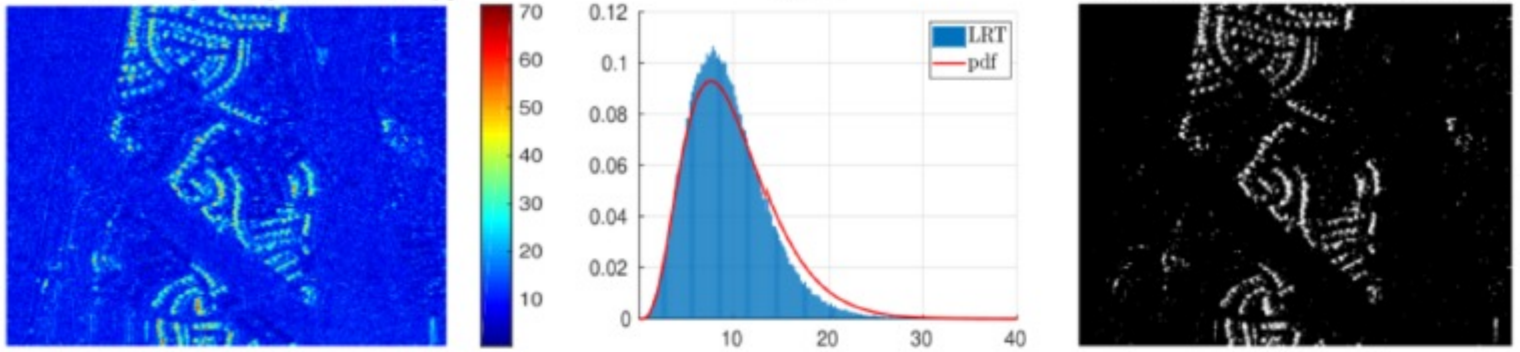

(a1'') τ_{LRT} (b1'') (c1'') LRT change detection map

Specified FAR(%)	Methods	Measured FAR (%)	Detection rate (%)	Overall error rate (%)
Scene 1				
0.5	DRT	1.71	40.77	10.65
	HLT	0.40	18.57	12.99
	LRT	0.41	20.26	12.74
1	DRT	2.43	45.16	10.58
	HLT	0.74	24.64	12.34
	LRT	0.64	24.40	12.29
5	DRT	6.78	57.06	12.41
	HLT	3.39	42.96	11.72
	LRT	2.74	37.95	11.96
10	DRT	11.37	63.38	15.30
	HLT	7.16	52.83	13.38
	LRT	6.04	46.65	13.39

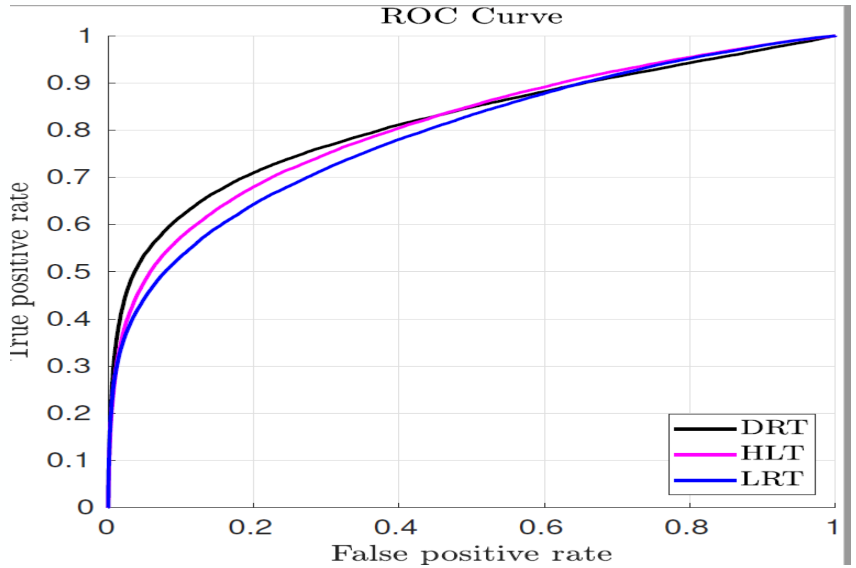

Conclusions

- Summary of the detectors and their characteristics

Characteristics	LRT	HLT	DRT
One sided or two sided	One sided	Two sided	Two sided
Statistical modeling	Approximate modeling	Approximate modeling	Exact distribution
Performance	fails for small number of looks	fails for small number of looks	Works better for small number of looks
Change detection direction	No	Yes	Yes

$$\mathbf{A} \sim \mathcal{RW}_d^{\mathbb{C}}(L_a, \Sigma_a) \text{ and } \mathbf{B} \sim \mathcal{RW}_d^{\mathbb{C}}(L_b, \Sigma_b).$$

$$H_0 : \Sigma_a = \Sigma_b \text{ and } L_a = L_b,$$
$$H_1 : \Sigma_a \neq \Sigma_b \text{ or/and } L_a \neq L_b.$$

- Future Work:
  - Extention of the method to model texture in the data
  - Omnibus test to mesure equality of several covariance matrices

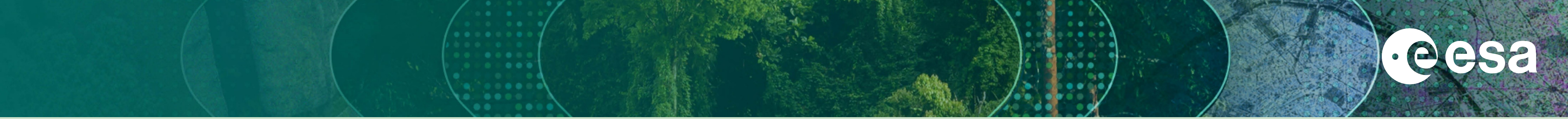
esa

Change Detection in Multilook Polarimetric SAR Imagery with Hotelling-Lawley Trace and Determinant Ratio Test Statistics

Thank you for your attention

Vahid Akbari
The University of Stirling
vahid.akbari@stir.ac.uk

POLINSAR AND BIOMASS 2023, Toulouse, 19th June 2023